AIAA JOURNAL
Vol. 43, No. 6, June 2005

Extension of Harten–Lax–van Leer Scheme for Flows at All Speeds

Hong Luo* and Joseph D. Baum†
Science Applications International Corporation, McLean, Virginia 22102
and
Rainald Löhner‡
George Mason University, Fairfax, Virginia 22030

The Harten, Lax, and van Leer with contact restoration (HLLC) scheme has been modified and extended in conjunction with time-derivative preconditioning to compute flow problems at all speeds. It is found that a simple modification of signal velocities in the HLLC scheme based on the eigenvalues of the preconditioned system is only needed to reduce excessive numerical diffusion at the low Mach number. The modified scheme has been implemented and used to compute a variety of flow problems in both two and three dimensions on unstructured grids. Numerical results obtained indicate that the modified HLLC scheme is accurate, robust, and efficient for flow calculations across the Mach-number range.

I. Introduction

HISTORICALLY, numerical algorithms for the solution of the Euler and Navier–Stokes equations are classified as either pressure-based or density-based solution methods. The pressure-based methods, originally developed and well suited for incompressible flows, are typically based on the pressure correction techniques. They usually use a staggered grid and solve the governing equations in a segregated manner. The density-based methods, originally developed and robust for compressible flows, use time-arching procedures to solve the hyperbolic system of governing equations in a coupled manner.

In general, density-based methods are not suitable for efficiently solving low Mach number or incompressible flow problems, because of large ratio of acoustic and convective timescales at the low-speed flow regimes. To alleviate this stiffness and associated convergence problems, time-derivative preconditioning techniques have been developed and used successfully for solving low-Mach-number and incompressible flows by many investigators, including Chorin,[1] Choi and Merkle,[2] Turkel,[3] Weiss and Smith,[4] and Dailey and Pletcher,[5] among others. Such methods seek to modify the time component of the governing equations so that the convergence can be made independent of Mach number. This is accomplished by altering the acoustic speeds of the system so that all eigenvalues become of the same order, and thus condition number remains bounded independent of the Mach number of the flows.

Over the last two decades characteristic-based upwind methods have established themselves as the methods of choice for prescribing the numerical fluxes for compressible Euler equations. When these upwind methods are used to compute the numerical fluxes for the preconditioned Euler equations, solution accuracy at low speeds can be compromised, unless the numerical flux formulation is modified to take into account the eigensystem of the preconditioned equations. Prior attempts in modifying Roe's flux-difference splitting scheme and advection upstream splitting method (AUSM) family flux-splitting schemes for flows at all speeds can be found in Refs. 4 and 6, respectively.

The Harten, Lax, and van Leer (HLL) scheme developed by Harten et al.[7] is attractive because of its robustness, conceptual simplicity, and ease of coding, but it has the serious flaw of diffusing contact surfaces. This is mainly because the HLL solver reduces the exact Riemann problem to two pressure waves and therefore neglects the contact surface. Toro et al.[8] discussed this limitation, and proposed a modified three waves solver, named HLLC, where the contact is explicitly presented. This HLLC scheme is found to have the following properties: 1) exact preservation of isolated contact and shear waves, 2) positivity preserving of scalar quantity, and 3) enforcement of entropy condition. The resulting scheme greatly improves contact resolution and has been successfully used to compute compressible viscous and turbulent flows on both structured grids[9] and unstructured grids.[10] The objective of the effort discussed in this paper is to progress the HLLC scheme toward a unified formulation suitable for accurate and efficient simulation of flow problems across the Mach-number range in conjunction with time-derivative preconditioning. It is found that a simple modification of signal velocities in the HLLC scheme based on the eigenvalues of the preconditioned system is only needed to reduce excessive numerical diffusion at the low Mach number. The preconditioned Euler and Navier–Stokes equations are solved using an implicit time-marching method on unstructured grids. The resulting system of linear equations is solved using a matrix-free generalized minimum residual+lower–upper symmetric Gauss–Seidel (GMRES+LU-SGS) method.[11,12] The modified HLLC scheme is used to compute inviscid fluxes at the interface. A variety of computations has been made for a wide range of flow conditions, for both inviscid and viscous flows, in both two and three dimensions to evaluate the accuracy and performance of the HLLC scheme. The numerical results obtained indicate that the modified HLLC scheme is accurate, simple, robust, and effective for flow calculations at all speeds.

II. Governing Equations

The Navier–Stokes equations governing unsteady compressible viscous flows can be expressed in the conservative form as

$$\frac{\partial \boldsymbol{U}}{\partial t} + \frac{\partial \boldsymbol{F}^j}{\partial \boldsymbol{x}_j} = \frac{\partial \boldsymbol{G}^j}{\partial \boldsymbol{x}_j} \tag{1}$$

where the summation convention has been employed. The flow variable vector $\boldsymbol{U}$, the inviscid flux vector $\boldsymbol{F}$, and viscous flux vector $\boldsymbol{G}$

Presented as Paper 2003-3840 at the 16th AIAA Computational Fluid Dynamics Conference, Orlando, FL, 23–26 June 2003; received 13 January 2004; revision received 8 October 2004; accepted for publication 27 October 2004.

*Senior Research Scientist, MS 2-6-9, Center for Applied Computational Sciences, 1710 SAIC Drive. Senior Member AIAA.
†Director, MS 2-6-9, Center for Applied Computational Sciences, 1710 SAIC Drive. Associate Fellow AIAA.
‡Professor, School of Computational Sciences, Institute for Computational Sciences and Informatics. Member AIAA.

are defined by

$$\boldsymbol{U} = \begin{pmatrix} \rho \\ \rho v_i \\ \rho e \end{pmatrix}, \quad \boldsymbol{F} = \begin{pmatrix} \rho v_j \\ \rho v_i v_j + p\delta_{ij} \\ v_j(\rho e + p) \end{pmatrix}$$

$$\boldsymbol{G} = \begin{pmatrix} 0 \\ \sigma_{ij} \\ v_l \sigma_{lj} + k\dfrac{\partial T}{\partial \boldsymbol{x}_j} \end{pmatrix} \tag{2}$$

Here ρ, p, e, T, and k denote the density, pressure, specific total energy, temperature, and thermal conductivity of the fluid, respectively, and v_i is the velocity of the flow in the coordinate direction x_i. Note that total energy is related to the total enthalpy H by $e = H - p/\rho$, where $H = h + |\boldsymbol{v}|^2/2$ and $h = C_p T$. Here, C_p is the specific heat at constant pressure. This set of equations is completed by the addition of the equation of state

$$p = (\gamma - 1)\rho\left(e - \tfrac{1}{2} v_j v_j\right), \qquad T = \left(e - \tfrac{1}{2} v_j v_j\right)\Big/ C_v \tag{3}$$

which is valid for perfect gas, where γ is the ratio of the specific heats and C_v is the specific heat at constant volume. The components of the viscous stress tensor σ_{ij} are given by

$$\sigma_{ij} = \mu\left(\frac{\partial v_i}{\partial x_j} + \frac{\partial v_j}{\partial x_i}\right) + \lambda \frac{\partial v_k}{\partial x_k}\delta_{ij} \tag{4}$$

The thermal conductivity k and viscosity coefficient μ are assumed to be a function of the temperature and are determined using Sutherland's empirical relation. It is assumed that λ and μ are related by Stokes's hypothesis

$$\lambda + 2\mu/3 = 0 \tag{5}$$

The left-hand side of Eq. (1) constitutes the Euler equations governing unsteady compressible inviscid flows.

III. Preconditioning System

The derivation of the preconditioned governing equations begins by transforming the original system of equations from the conservative variables $\boldsymbol{U}$ to the primitive variables $\boldsymbol{Q}$ as follows:

$$\frac{\partial \boldsymbol{U}}{\partial \boldsymbol{Q}}\frac{\partial \boldsymbol{Q}}{\partial t} + \frac{\partial \boldsymbol{F}^j}{\partial \boldsymbol{x}_j} = \frac{\partial \boldsymbol{G}^j}{\partial \boldsymbol{x}_j} \tag{6}$$

where $\boldsymbol{Q} = [p, v_x, v_y, v_z, T]^t$ and Jacobian $\partial \boldsymbol{U}/\partial \boldsymbol{Q}$ is given by

$$\frac{\partial \boldsymbol{U}}{\partial \boldsymbol{Q}} = \begin{pmatrix} \rho_p & 0 & 0 & 0 & \rho_T \\ \rho_p v_x & \rho & 0 & 0 & \rho_T v_x \\ \rho_p v_y & 0 & \rho & 0 & \rho_T v_y \\ \rho_p v_z & 0 & 0 & \rho & \rho_T v_z \\ \rho_p H - 1 & \rho v_x & \rho v_y & \rho v_z & \rho_T H + \rho C_p \end{pmatrix} \tag{7}$$

with

$$\rho_p = \left.\frac{\partial \rho}{\partial p}\right|_T, \qquad \rho_T = \left.\frac{\partial \rho}{\partial T}\right|_p \tag{8}$$

The preconditioned Navier–Stokes equations are then obtained by replacing the original nonpreconditioned Jacobian matrix $\partial \boldsymbol{U}/\partial \boldsymbol{Q}$ with a preconditioning matrix Γ:

$$\Gamma\frac{\partial \boldsymbol{Q}}{\partial t} + \frac{\partial \boldsymbol{F}^j}{\partial \boldsymbol{x}^j} = \frac{\partial \boldsymbol{G}^j}{\partial \boldsymbol{x}^j} \tag{9}$$

The following preconditioning matrix Γ, originally proposed by Choi and Merkle[2] and extended further by Weiss and Smith,[4] is used in the present work:

$$\Gamma = \begin{pmatrix} \Theta & 0 & 0 & 0 & \rho_T \\ \Theta v_x & \rho & 0 & 0 & \rho_T v_x \\ \Theta v_y & 0 & \rho & 0 & \rho_T v_y \\ \Theta v_z & 0 & 0 & \rho & \rho_T v_z \\ \Theta H - 1 & \rho v_x & \rho v_y & \rho v_z & \rho_T H + \rho C_p \end{pmatrix} \tag{10}$$

where Θ is given by

$$\Theta = \left(1\Big/ V_r^2 - \rho_T/\rho C p\right) \tag{11}$$

Here V_r is a reference velocity. The choice of the reference velocity V_r is crucial for success of the preconditioning method. If the magnitude of the reference velocity is equal to the local speed of sound, the preconditioned system (9) recovers to the nonpreconditioned system (1). To make all eigenvalues of preconditioned system (1) have the same order of magnitude, the reference velocity must be of the same order as a local velocity. In this work, the following reference velocity V_r is used:

$$V_r = \min[c, \max(|\boldsymbol{v}|, K|\boldsymbol{v}_\infty|)] \tag{12}$$

where $|\boldsymbol{v}|$ is the local velocity magnitude, $|\boldsymbol{v}_\infty|$ is a fixed reference velocity, c is the speed of sound, and K is a constant. Note that following Turkel[3] the reference velocity V_r in Eq. (12) is limited to prevent anomalous behavior at the near-stagnation conditions. In the present work, $|\boldsymbol{v}_\infty|$ is set to be the freestream velocity and K is fixed at 0.5.

For the low-Reynolds-number viscous flows, the reference velocity should not be smaller than the local diffusion velocity $\mu/\rho\Delta d$, where Δd is the characteristic mesh size length. Thus,

$$V_r = \max(V_r, \mu/\rho\Delta d) \tag{13}$$

The resultant eigenvalues of the preconditioned system are given by

$$\lambda\left(\Gamma^{-1}\frac{\partial \boldsymbol{F}}{\partial \boldsymbol{Q}}\right) = v' - c', v_n, v_n, v_n, v' + c' \tag{14}$$

where

$$v_n = \boldsymbol{v} \cdot \boldsymbol{n} \tag{15}$$

$$v' = v_n(1 - \alpha) \tag{16}$$

$$c' = \sqrt{\alpha^2 v_n^2 + V_r^2} \tag{17}$$

$$\alpha = \left(1 - \beta V_r^2\right)\Big/ 2 \tag{18}$$

$$\beta = \rho_p + \rho_T/\rho C_p \tag{19}$$

Here $\boldsymbol{n}$ denotes the unit outward normal vector to the interface. Note that all eigenvalues remain of the order of v as long as the reference velocity is of the same order as the local velocity.

IV. Preconditioned HLLC Scheme

Over the past two decades characteristic-based upwind methods have established themselves as the methods of choice for prescribing the numerical fluxes for compressible Euler equations. When these upwind methods are used to compute the numerical fluxes for the preconditioned Euler equations, solution accuracy at low speeds can be compromised, unless the numerical flux formulation is modified to take into account the eigensystem of the preconditioned equations. The particular version of the HLLC scheme is defined in Ref. 9 and can be easily modified to operate effectively at very low Mach numbers by replacing the signal velocities with the preconditioned

signal velocities. The inviscid interface flux computed using the preconditioned HLLC scheme can be expressed as

$$\boldsymbol{F}_{ij}^{\mathrm{HLLC}} = \begin{cases} \boldsymbol{F}_i, & \text{if} \quad S_i > 0 \\ \boldsymbol{F}(\boldsymbol{U}_i^*), & \text{if} \quad S_i \le 0 < S_M \\ \boldsymbol{F}(\boldsymbol{U}_j^*), & \text{if} \quad S_M \le 0 \le S_j \\ \boldsymbol{F}_j, & \text{if} \quad S_j < 0 \end{cases} \tag{20}$$

where

$$\boldsymbol{U}_i^* = \begin{pmatrix} \rho_i^* \\ (\rho \boldsymbol{v})_i^* \\ (\rho E)_i^* \end{pmatrix} = \frac{1}{S_i - S_M} \begin{pmatrix} (S_i - v_{n_i})\rho_i \\ (S_i - v_{n_i})(\rho \boldsymbol{v})_i + (p^* - p_i)\boldsymbol{n} \\ (S_i - v_{n_i})(\rho E)_i - p_i v_{n_i} + p^* S_M \end{pmatrix} \tag{21}$$

$$\boldsymbol{U}_j^* = \begin{pmatrix} \rho_j^* \\ (\rho \boldsymbol{v})_j^* \\ (\rho E)_j^* \end{pmatrix} = \frac{1}{S_j - S_M} \begin{pmatrix} (S_j - v_{n_j})\rho_j \\ (S_j - v_{n_j})(\rho \boldsymbol{v})_j + (p^* - p_j)\boldsymbol{n} \\ (S_j - v_{n_j})(\rho E)_j - p_j v_{n_j} + p^* S_M \end{pmatrix} \tag{22}$$

$$\boldsymbol{F}_i^* \equiv \boldsymbol{F}(\boldsymbol{U}_i^*) = \begin{pmatrix} S_M \rho_i^* \\ S_M (\rho \boldsymbol{v})_i^* + p^* \boldsymbol{n} \\ S_M ((\rho E)_i^* + p^*) \end{pmatrix} \tag{23}$$

$$\boldsymbol{F}_j^* \equiv \boldsymbol{F}(\boldsymbol{U}_j^*) = \begin{pmatrix} S_M \rho_j^* \\ S_M (\rho \boldsymbol{v})_j^* + p^* \boldsymbol{n} \\ S_M ((\rho E)_j^* + p^*) \end{pmatrix} \tag{24}$$

$$\begin{aligned} p^* &= \rho_i \left(v_{n_i} - S_i\right)\left(v_{n_i} - S_M\right) + p_i \\ &= \rho_j \left(v_{n_j} - S_j\right)\left(v_{n_j} - S_M\right) + p_j \end{aligned} \tag{25}$$

and S_M is defined as

$$S_M = \frac{\rho_j v_{n_j}\left(S_j - v_{n_j}\right) - \rho_i v_{n_i}\left(S_i - v_{n_i}\right) + p_i - p_j}{\rho_j \left(S_j - v_{n_j}\right) - \rho_i \left(S_i - v_{n_i}\right)} \tag{26}$$

Signal velocities S_i and S_j are defined as

$$S_i = \min(v_i' - c_i', \hat{v}' - \hat{c}') \tag{27}$$

$$S_j = \max(v_j' + c_j', \hat{v}' + \hat{c}') \tag{28}$$

with $\hat{v}'$ and $\hat{c}'$ being Roe's average variables for preconditioned velocity and speed of sound. The only modification made in the HLLC scheme is that the signal velocities S_i and S_j are now defined using the preconditioned eigenvalues. This modification is based on the promise that the dissipative contributions should be scaled by the velocity magnitude, rather than by the speed of sound, as the local Mach number decreases. Note that in the supersonic regions, where $\alpha = 0$, $V_r = c$, $c' = c$, $v' = v_n$, the preconditioned HLLC scheme recovers to the original HLLC scheme.

V. Numerical Results

The modified HLLC formulation has been incorporated into a unstructured grid Navier–Stokes solver with turbulence modeling capability,[10,11] where the mean-flow and turbulence-model equations are decoupled in the time integration in order to facilitate the incorporation of different turbulence models. The one-equation turbulence model developed by Spalart and Allmaras[13] is used to compute turbulent flows in the present work. Both preconditioned mean-flow equations and turbulence model are integrated in time using an implicit scheme. The resulting system of linear equations is solved using a matrix-free GMRES+LU-SGS method.[11] The spatial discretizations are carried out using a hybrid finite volume and finite element method, where a finite volume approximation is used to discretize the inviscid fluxes, and a Galerkin finite element approximation with piecewise linear elements is used to evaluate the viscous flux terms. The numerical flux functions for inviscid fluxes at the dual mesh cell interface are computed using the modified HLLC scheme. The high-order accuracy in space is achieved using

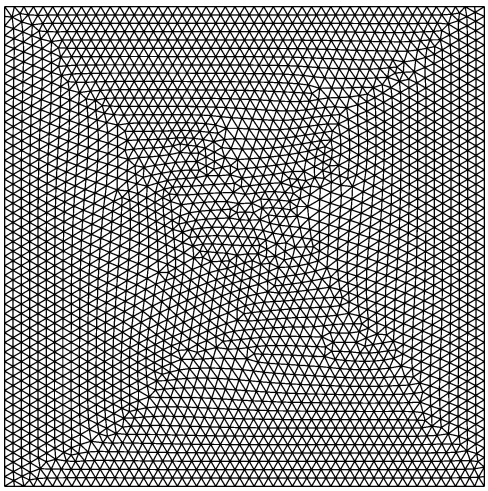

Fig. 1a Mesh for lid-driven cavity problem.

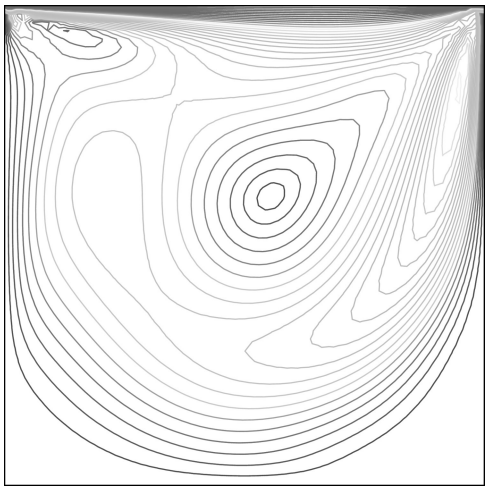

Fig. 1b Computed velocity contours for lid-driven cavity problem at $M_\infty = 0.005$, $Re = 400$.

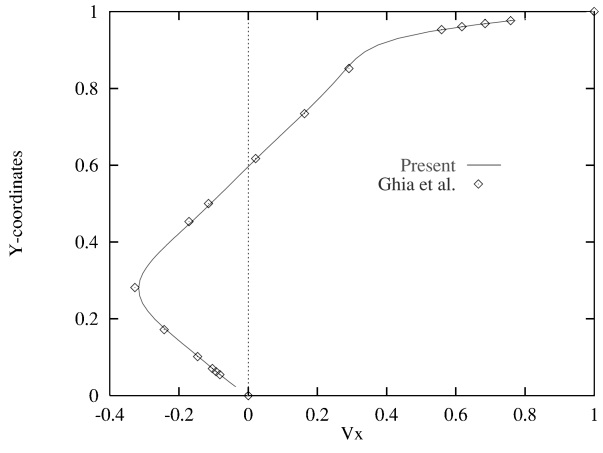

Fig. 1c Computed X-direction velocity distribution along vertical geometric centerline at $M_\infty = 0.005$, $Re = 400$.

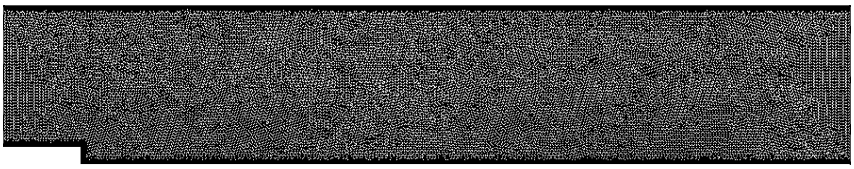

Fig. 2a Mesh for backward-facing step ($n$elem = 135,832; $n$poin = 72,434; $n$boun = 9034).

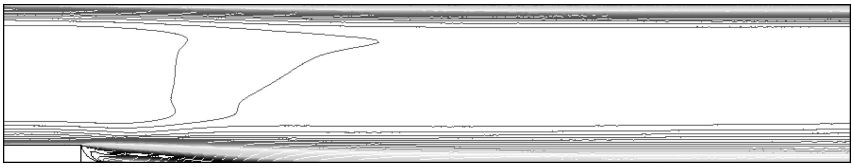

Fig. 2b Computed Mach-number contours for backward-facing step problem at $M_\infty = 0.128$, $Re = 33.42 \times 10^3$.

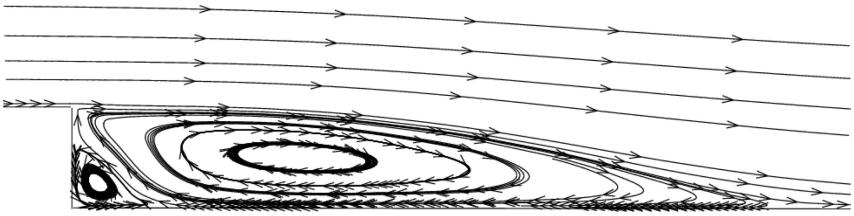

Fig. 2c Computed velocity streamline traces for backward-facing step problem at $M_\infty = 0.128$, $Re = 33.42 \times 10^3$.

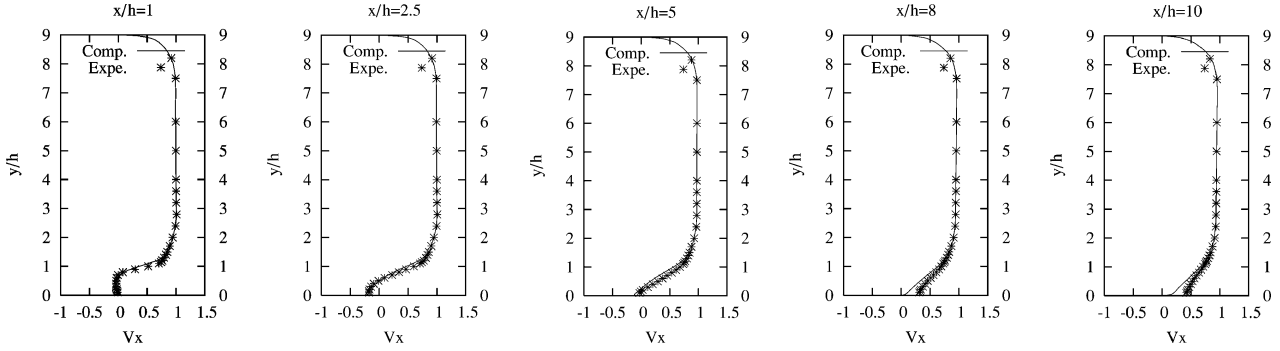

Fig. 2d Comparison of streamwise velocity profiles at selected locations for backward-facing step problem at $M_\infty = 0.128$, $Re = 33.42 \times 10^3$.

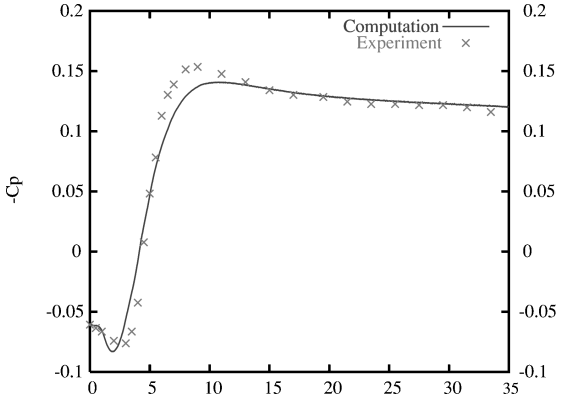

Fig. 2e Comparison of pressure coefficient distribution on the bottom wall for backward-facing step problem at $M_\infty = 0.128$, $Re = 33.42 \times 10^3$.

a reconstruction algorithm based on the primitive variables and monotone upwind schemes for scalar conservation laws approach. The developed method has been validated and verified for a number of benchmark test cases. A grid-convergence study indicates that the present algorithm is second-order accurate in space. Only a few typical examples are presented here to demonstrate the accuracy, effectiveness, and robustness of the present method.

A. Lid-Driven Cavity Flow

The two-dimensional lid-driven cavity flow problem was studied extensively and served as a benchmark test case for the incompressible Navier–Stokes calculations. This test case is chosen to study the accuracy and effectiveness of the developed method for low-Reynolds-number viscous flows. The grid used in the computation is shown in Fig. 1a. It contains 5398 elements, 2800 grid points, and 200 boundary points. The computation was performed at a Mach number of 0.005 and a Reynolds number of 400. Figure 1b shows the computed velocity in the flowfield. The u-velocity component along the vertical centerline is shown in Fig. 1c. The solution of Ghia et al.,[14] which is considered a standard benchmark solution, used a very fine 129×129 grid points and is also shown for comparison. The virtually identical agreement indicates that the present method yields very accurate solution to the low-Reynolds-number incompressible Navier–Stokes equations.

B. Turbulent Backward-Facing Step Flow

The second validation case was the turbulent flow computation around a backward-facing step. The configuration of the backward-facing step is that of Ref. 15: the expansion ratio (channel inlet height:channel outlet height) is 1:1.125. Figure 2a shows a view of the grid used in the computation. It contains 135,832 elements; 72,434 grid points; and 9034 boundary points. The computational domain extends four step heights upstream of the step and 40 step heights downstream from the step. Inlet Mach number is 0.128, and the Reynolds number based on the step height and inlet velocity is 33.42×103. Such a high Reynolds number is used to ensure that the boundary layer is entirely turbulent prior to passing over the step. Figure 2b shows the plot of Mach-number contours. A close-up view of the particle traces based on the streamwise velocity is shown in Fig. 2c, where one can clearly see the separation region

along with the corner eddy and reattachment region. The streamwise velocity profiles at various axial locations are compared with those of the experimental data in Fig. 2d and show very good agreement. A plot of the pressure coefficient distribution for the bottom wall is shown in Fig. 2e and again shows fairly good agreement with the experimental results. The observed discrepancy between the computed solution and the experimental data might be caused by the one-equation turbulence model used in the present calculation, where the accurate modeling of large separations is still a big challenge. Nevertheless, this test case clearly demonstrates the accuracy and robustness of the modified HLLC scheme for predicting separated turbulent flows at the low Mach number.

C. Transonic Flow past RAE2822 Airfoil

The third test case was a simulation of transonic flow over a RAE2822 airfoil at a Mach number of 0.73, a chord Reynolds number of 6.5×10^6, and an incidence of 2.8 deg. The flow condition is denoted as test case 9 in the experimental report by Cook et al.[16] This test case is chosen to demonstrate the accuracy and performance of the present method for solving transonic flow problems. The mesh used in the computation shown in Fig. 3a contains 25,172 elements; 12,741 points; and 310 boundary points. The computed Mach number and pressure contours in the flowfield are displayed in Figs. 3b and 3c, respectively. A shock wave forms at about 55% on the upper surface. The computed eddy viscosity is depicted in Fig. 3d. A smooth distribution of eddy viscosity throughout the boundary layer and vanishingly small values in the inviscid regions of flow are observed. The computed surface-pressure and skin-friction distributions are compared with experimental data[16] in Figs. 3e and 3f,

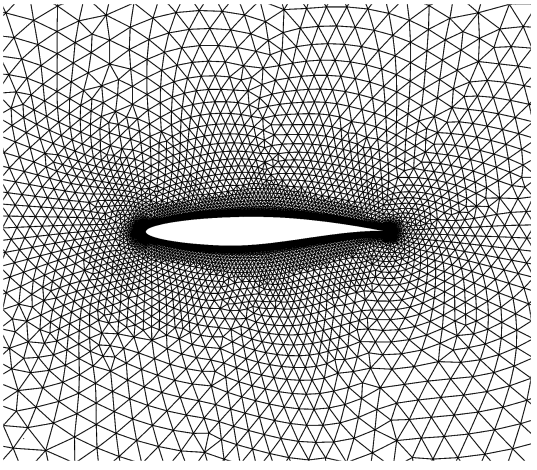

Fig. 3a Unstructured mesh used for computing turbulent flow over a RAE2822 airfoil (*n*elem = 25,172; *n*poin = 12,741; *n*boun = 310).

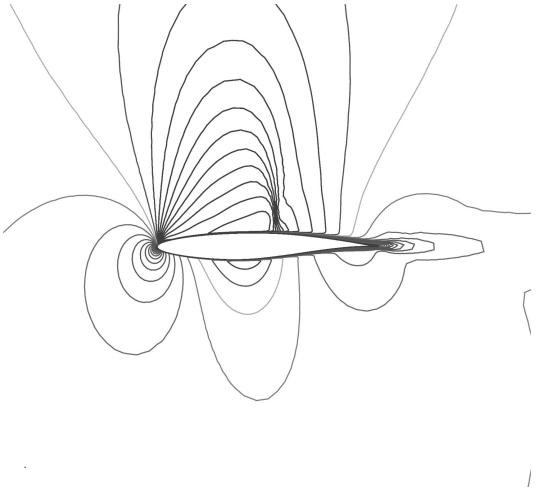

Fig. 3b Computed Mach-number contours for turbulent flow over a RAE2822 airfoil ($M_\infty = 0.73$, $Re = 6.5 \times 10^6$, $\alpha = 2.8$ deg).

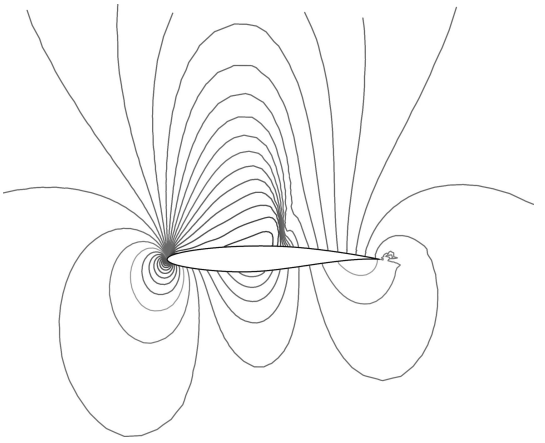

Fig. 3c Computed pressure contours for turbulent flow over a RAE2822 airfoil ($M_\infty = 0.73$, $Re = 6.5 \times 10^6$, $\alpha = 2.8$ deg).

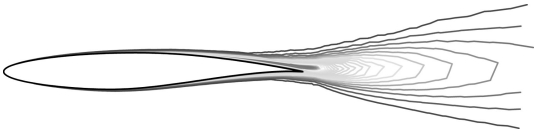

Fig. 3d Computed eddy-viscosity contours for turbulent flow over a RAE2822 airfoil ($M_\infty = 0.73$, $Re = 6.5 \times 10^6$, $\alpha = 2.8$ deg).

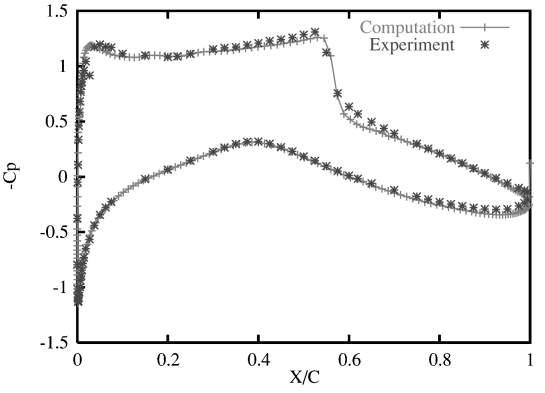

Fig. 3e Comparison of computed surface-pressure coefficient with experimental data for turbulent flow over a RAE2822 airfoil.

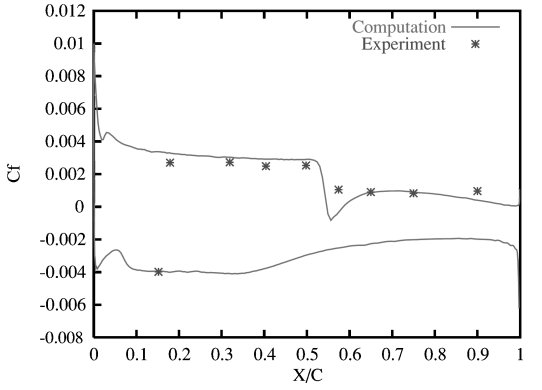

Fig. 3f Comparison of computed skin-friction coefficient with experimental data for turbulent flow over a RAE2822 airfoil.

respectively, indicating an overall good agreement. The computed lift coefficient of 0.801 and drag coefficient of 0.0160 are compared favorably with the experimental values of 0.803 and 0.0168, respectively.

D. Inviscid Flow past a Sphere

Inviscid flow past a sphere at a Mach number of 0.005 is computed in this test case to demonstrate the accuracy and effectiveness

of the developed method for three-dimensional problems. Because of the symmetrical nature of this problem, only a quarter of a sphere was calculated. The mesh, which contains 73,397 elements, 14,281 grid points, and 3479 boundary points, is depicted in Fig. 4a. The computed velocity in the flowfield is shown in Fig. 4b. Figure 4c illustrates the velocity distributions obtained by the solutions with and without preconditioning and the pressure-based incompressible solution. The analytical solution is also shown in the figure for comparison. The solution without preconditioning was severely degraded, as the excess diffusion in the original system corrupts the solution. The result obtained using the present preconditioning method is comparable to, if not better than, the one using the pressure-based incompressible method developed by the present authors.[17] This test case clearly demonstrates the accuracy of the present method for the three-dimensional problem.

E. Viscous Flow past an Open-Wheel Race Car

As an example of application, the developed method has been used to compute viscous flow past an open-wheel race car (e.g., the flow over rotating wheels). The computation was performed at a freestream Mach number of 0.13134 and a Reynolds number of 1×10^6. The mesh used in the computation, shown in Fig. 5a, assumes a symmetrical model and contains 8,314,454 elements; 1,459,199 grid points; and 173,134 boundary points. The computed velocity and streamline trace in the flowfield nearby the car model are presented in Figs. 5b and 5c, respectively. The pressure distribution on the moving ground plane centerline between the experimental data and computational result is displayed in Fig. 5d.

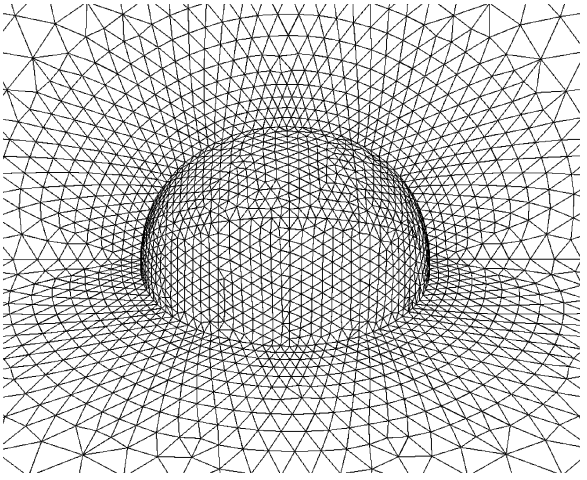

Fig. 4a Surface mesh used for computing flow past a sphere (*n*elem = 73,397; *n*poin = 14,281; *n*boun = 3479).

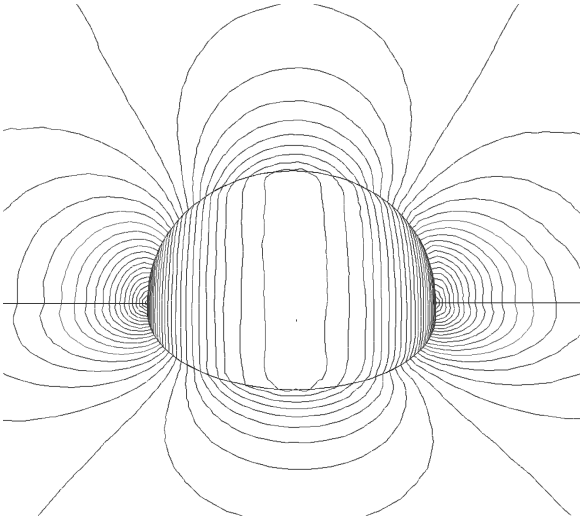

Fig. 4b Computed velocity contours on the surface of the sphere at $M_\infty = 0.005$ and $\alpha = 0.0$.

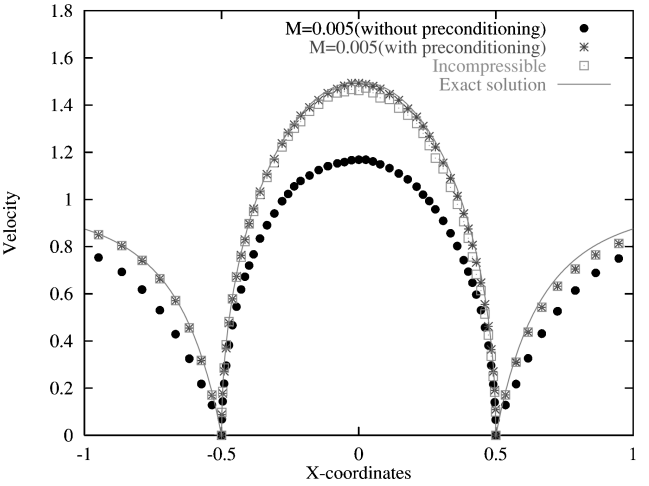

Fig. 4c Comparison of velocity profiles obtained by different numerical methods.

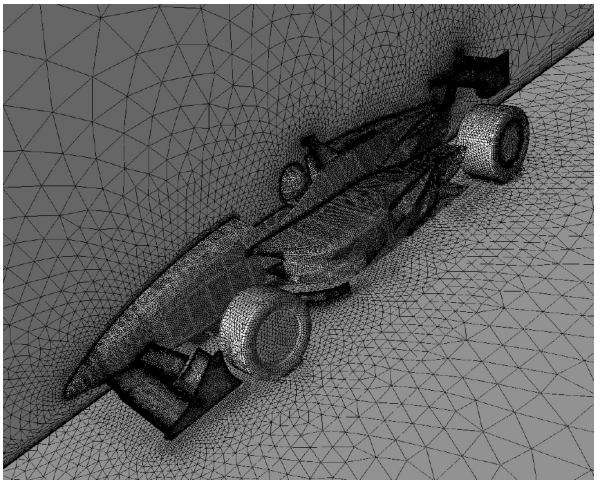

Fig. 5a Surface mesh used for computing laminar flow past an open-wheel race car (*n*elem = 8,314,454; *n*poin = 1,459,199; *n*boun = 173,134).

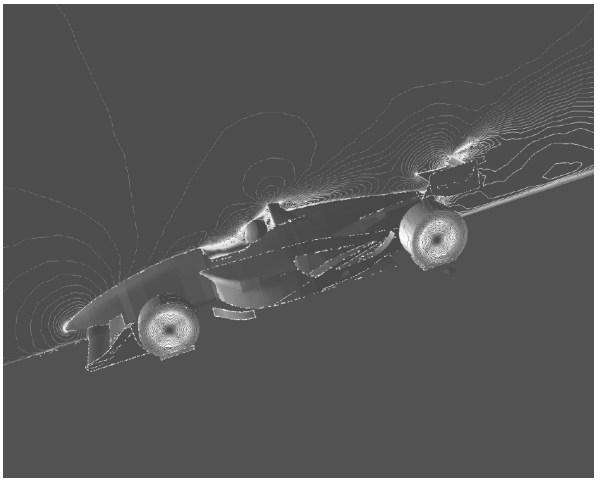

Fig. 5b Computed velocity contours on the surface of the race car at $M_\infty = 0.13134$, $\alpha = 0.0$, and $Re = 10^6$.

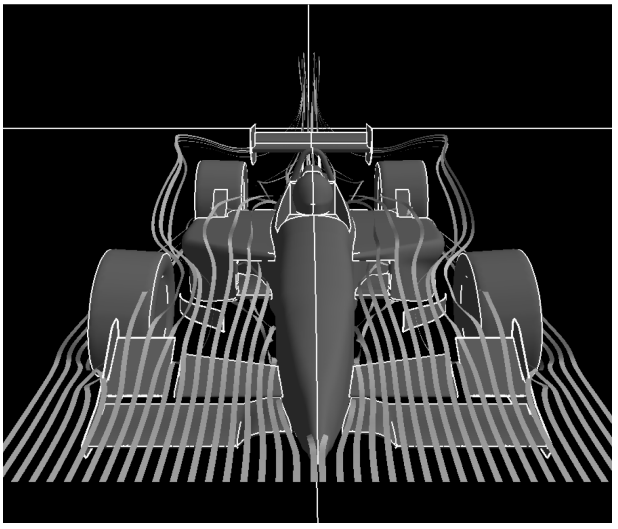

Fig. 5c Computed streamline trace in the flowfield near the race car at $M_\infty = 0.13134$, $\alpha = 0.0$, and $Re = 10^6$.

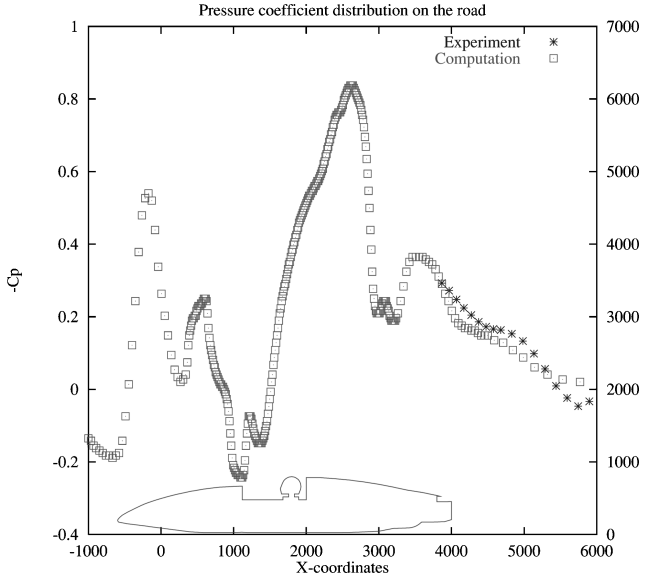

Fig. 5d Comparison of pressure coefficient distribution on the road between the computational result and experimental data.

VI. Conclusions

The Harten, Lax, and van Leer (HLLC) scheme has been modified and extended to compute the flows at all speeds in conjunction with time-derivative preconditioning technique. The developed methods have been used to simulate a wide variety of flow types and speeds. The numerical results indicate that the slightly modified but nonetheless simple formulation of the HLLC scheme is effective in maintaining solution accuracy and efficiency for flow calculations at all speeds.

References

[1]Chorin, J., "A Numerical Method for Solving Incompressible Viscous Flow Problems," *Journal of Computational Physics*, Vol. 2, No. 1, 1967, pp. 12–26.

[2]Choi, Y. H., and Merkle, C. L., "The Application of Preconditioning in Viscous Flows," *Journal of Computational Physics*, Vol. 105, No. 2, 1993, pp. 207–223.

[3]Turkel, E., "Preconditioned Methods for Solving the Incompressible and Low Speed Compressible Equations," *Journal of Computational Physics*, Vol. 72, No. 2, 1987, pp. 277–298.

[4]Weiss, J. M., and Smith, W. A., "Preconditioning Applied to Variable and Constant Density Time-Accurate Flows on Unstructured Meshes," *AIAA Journal*, Vol. 33, No. 11, 1995, pp. 2050–2057.

[5]Dailey, L. D., and Pletcher, R. H., "Evaluation of Multigrid Acceleration for Preconditioned Time-Accurate Navier–Stokes Algorithms," AIAA Paper 95-1668, Jan. 1995.

[6]Edwards, J. R., and Liou, M. S.,"Low-Diffusion Flux-Splitting Methods for Flows at All Speeds," *AIAA Journal*, Vol. 36, No. 9, 1998, pp. 1610–1617.

[7]Harten, A., Lax, P. D., and van Leer, B., "On Upstream Differencing and Godunov-Type Scheme for Hyperbolic Conservation Laws," *SIAM Review*, Vol. 25, No. 1, 1983, p. 35.

[8]Toro, E. F., Spruce, M., and Speares, W., "Restoration of the Contact Surface in the HLL Riemann Solver," *Shock Waves*, Vol. 4, No. 25, 1994, pp. 25–34.

[9]Batten, P., Leschziner, M. A., and Goldberg, U. C., "Average-State Jacobians and Implicit Methods for Compressible Viscous and Turbulent Flows," *Journal of Computational Physics*, Vol. 137, No. 1, 1997, pp. 38–78.

[10]Luo, H., Baum, J. D., and Löhner, R., "High-Reynolds Number Viscous Flow Computations Using an Unstructured-Grid Method," AIAA Paper 2004-1104, 2004; also *Journal of Aircraft*, Vol. 42, No. 2, 2005, pp. 483–492.

[11]Luo, H. D., Baum, J. D., and Löhner, R., "A Fast, Matrix-Free Implicit Method for Compressible Flows on Unstructured Grids," *Journal of Computational Physics*, Vol. 146, No. 2, 1998, pp. 664–690.

[12]Luo, H. D., Baum, J. D., and Löhner, R., "A Fast, Matrix-Free Implicit Method for Computing Low Mach Number Flows Flows on Unstructured Grids," *International Journal of Computational Fluid Dynamics*, Vol. 14, 2001, pp. 135–157.

[13]Spalart, P. R., and Allmaras, S. R., "A One-Equations Turbulence Model for Aerodynamic Flows," AIAA Paper 92-0439, Jan. 1992.

[14]Ghia, U., Ghia, K. N., and Shin, C. T., "High-Re Solution for Incompressible Flow Using the Navier–Stokes Equations and a Multigrid Method," *Journal of Computational Physics*, Vol. 48, No. 3, 1982, pp. 387–411.

[15]Driver, D. M, and Seegmiller, H. L., "Features of Reattaching Turbulent Shear Layer in Divergent Channel Flow," *AIAA Journal*, Vol. 23, No. 2, 1985, pp. 163–171.

[16]Cook, P. H., McDonald, M. A., and Firmin, M. C. P., "Aerofoil RAE 2822 Pressure Distributions, and Boundary Layer and Wake Measurements," AGARD, Advisory Rept. 138, May 1979.

[17]Luo, H. D., Baum, J. D., and Löhner, R., "A Finite Volume Scheme for Hydrodynamic Free Boundary Problems on Unstructured Grids," AIAA Paper 95-0668, 1995.

C. Kaplan
Associate Editor